Modeling and Analysis of Machinability Evaluation in the Powder Mixed Electrical Discharge Machining of Cobalt-Bonded Tungsten Carbide

Ko-Ta Chiang, Fu-Ming Chang, Nun-Ming Liu, Chih-Chung Chou

Abstract

For the powder mixed electrical discharge machining (PM-EDM) process, the aluminum powder particle suspended in the dielectric fluid disperses and uniforms the discharging energy dispersion, and displays multiple discharging effects within a single input pulse. The objective of this paper was to present the mathematical models for modeling and analysis of the effects of processing parameters, including the discharge current, pulse on time, grain size and concentration of aluminum powder particle, on the machinability evaluation in terms of material removal rate (MRR), electrode wear ratio (EWR) and surface roughness (SR) in the PM-EDM process of cobalt-bonded tungsten carbide. An experimental plan of a central composite design (CCD) based on the response surface methodology (RSM) was employed to carry out the experimental study. This study highlighted the development of mathematical models for investigating the influences of

Ko-Ta Chiang, Professor, Department of Mechanical Engineering, Hsiuping University of Science and Technology
Fu-Ming Chang, Associate Professor, Department of Mechanical Engineering, Hsiuping University of Science and Technology
Nun-Ming Liu, Assistant Professor, Department of Mechanical Engineering, Hsiuping University of Science and Technology
Chih-Chung Chou, Lecturer, Department of Mechanical Engineering, Hsiuping University of Science and Technology
Received 13 March 2015; accepted 25 June 2015

processing parameters on the machinability evaluation, and the proposed mathematical models in this study had proven to fit and predict values of performance characteristics close to those readings recorded experimentally with a 95% confidence interval. Results show that the effect of aluminum powder particle added in the dielectric fluid promotes both the values of MRR and EWR, simultaneously. The value of SR decreases with an increase of powder concentration, and increases with an increase of grain size for various powder concentrations. The discharge current and the pulse on time have statistically significant on the values of MRR, EWR and SR.

Keywords: Modeling, powder mixed electrical discharge machining, machinability evaluation, Response surface methodology

碳化鎢於粉末混合放電加工過程中加工性能之建模與分析

江可達、張浮明、劉南明、周志忠

摘要

對於粉末混合放電加工過程中，添加於介電液中的鋁粉末具有對於放電能量的分散與均化作用，使得單一輸入的放電脈衝呈現有放大其放電能量的效應。本文的研究目的是呈現一數學模組用於建模與分析其放電加工參數，包含有放電電流、脈衝時間、鋁粉的顆粒大小與濃度等，對於碳化鎢於粉末混合放電加工過程中加工性能如材料移除率、電極消耗率與表面粗糙度等的影響。實驗規劃上採用反應曲面法為基礎的中央組合法來進行實驗的研究。本文著重於數學模組的開發用於探討其放電加工參數對於加工性能的影響，所提的數學模組獲得證實可吻合與預測其加工性能並有 95%可靠度接近其實驗值。結果顯示，添加於介電液中的鋁粉末具有同時提升其材料移除率、電極消耗率的數值。其表面粗糙度會隨著鋁粉的濃度增加而減少，卻隨著鋁粉的顆粒增大而增加。而放電電流、脈衝時間對於材料移除率、電極消耗率與表面粗糙度等的加工性能皆有統計上明顯的影響。

關鍵詞：建模、粉末混合放電加工、加工性能、反應曲面法

江可達：修平科技大學機械工程系教授
張浮明：修平科技大學機械工程系副教授
劉南明：修平科技大學機械工程系助理教授
周志忠：修平科技大學機械工程系講師
投稿日期：104 年 3 月 13 日　接受刊登日期：104 年 6 月 25 日

1. Introduction

Electrical discharge machining (EDM) process is an electrical spark-erosion process which removes workpiece material by means of a series of recurring electrical spark. The discharging sparks occur between the electrode and electro-conductive workpiece flushed with or submerged in a dielectric fluid. The EDM process has the advantage of spark-erosion in order to machine the hard-to-cut material and then easily achieve the required shapes and sizes with enhancing machining productivity and better dimensional accuracy [1, 2]. Since it has more versatile benefits, the EDM has been widely applied in modern metal industry for producing complex cavities in moulds and dies, which are difficult to manufacture by conventional machining. However, the material removal mechanism is achieved by the melting and evaporation of workpiece material at each electrical discharge spot, which are then ejected and flushed away by the dielectric fluid. Due to the rapid high temperature melting and cooling process, subsurface defects such as cracks, spall, porosity, residual stress, metallurgical transformations and heat affected zones (HAZ) are easily found on the machined surface of workpiece [3-5]. For restoring the machined surface properties and removing the surface detects, the technique of fine abrasive powder mixed into the dielectric fluid of EDM, called as the powder mixed EDM (PM-EDM), is thus proposed.

Erden and Bilgin [6] first studied the effects of abrasive/metallic powder (copper, aluminum, iron and carbon) mixed into the dielectric fluid of EDM, and proposed that the machining rate increased with the increases of the powder concentration due to decreasing the time lag. Jeswani [7] presented that the material removal rate was improved around 60% and electrode wear ratio was reduced about 15% by using the kerosene oil mixed with 4 g/l graphite powder as dielectric fluid in the EDM process. Mohri et al. [8], Yan and Chen [9], and Uno and Okada [10] investigated the effects of silicon powder addition on machining rate and surface roughness in EDM. Wong et al. [11], Furutani et al. [12] and Yan et al. [13] suggested that the machined surface properties, including hardness, wear resistance and corrosion resistance could be significantly improved by using the PM-EDM process. Wu [14] discussed the improvement of the machined surface of EDM by adding aluminum powder and surfactant into dielectric fluid. Kansal [15] had made to optimize the process parameters

of PM-EDM by using the response surface methodology. The literature of the above reveals that the additive powder particle reduces the insulating strength of the dielectric fluid and disperses the discharging energy dispersion; these advantages improve the material removal and refine the machined surface roughness.

The cobalt-bonded tungsten carbide is a kind of high strength and difficult-cutting material, which is produced by compacting techniques of powder metallurgy and high-temperature sintering. Although the major portion of machining applications of this type of cemented tungsten carbide is used as cutting tools, the scope of alternative applications is quickly growing such as moulding material of metal forming, forging, squeeze casting and high pressure die casting. In the conventional EDM process, the machined surface easily produces large amount of cracks and spall to cause the decrease of hardness, wear resistance and corrosion resistance. Hence, the present study attempted using the technique of PM-EDM for machining the cobalt-bonded tungsten carbide material. This paper highlighted the development of mathematical models for modeling and correlates the inter-relationship of various processing parameters on the machinability evaluation of cobalt-bonded tungsten carbide in the PM-EDM process through the response surface methodology (RSM). The RSM is an empirical modeling approach for determining the relationship between various processing parameters and responses with the various desired criteria, and it is used to search out the significance of these processing parameters on the coupled responses [16]. It is one of the most widely used methods to solve the optimization problem in the manufacturing environments [17-19]. In this study, the effects of various processing parameters on the machinability evaluation in terms of material removal rate (MRR), electrode wear ratio (EWR) and surface roughness (SR) were systematically investigated.

2. Experimental procedure

2.1 Equipment and specimen material

A series of experiments were performed on a die-sinking CNC EDM machine of type OMEGA-CM43 with a dielectric cycling system. Various aluminum powder particles were suspended into the dielectric fluid. The dielectric cycling system maintained a uniform distribution of the added powder particles by using the cycling

capability. Commercial-grade mineral oil (TOTAL EDM44) with a flash point of 85°C was used as the dielectric fluid and the side injection of dielectric fluid was adopted. A jet flushing system was employed to assure adequate flushing of the EDM process debris from the gap zone. The electrolytic copper with diameter 25 mm was used as an electrode. The physical and mechanical properties of electrolytic copper are a melting point of 1,360K, density of 8.94 g/cm3, thermal conductivity of 226 W/mK and electrical resistivity of 17.1 nΩm. According to the bibliography in the EDM field and the results of related experiments, the electrode used in this study was subjected to a negative polarity in order to ensure the promotion of good surface quality [1-3].

The workpiece material used in this study is cobalt-bonded tungsten carbide (96WC-4Co, manufacturer: Protool Industrial Co.), which is composed of approximate (96%) of tungsten carbide (WC) and (4%) of cobalt (Co). This material was frequently used for the cutting tools due to its excellent hardness properties (HRA 93.8). Furthermore, it possesses a high compressive strength (6.6 kN/mm^2), as well as good resistance of wear and oxidation at high temperature status. The compound materials of tungsten carbide were mixed with cobalt (Co) in a certain proportion in order to provide a high resistance to thermal shock. It has a thermal conductivity of 100 W/mK and a thermal expansion coefficient of $4.3\times10^{-6}K^{-1}$ at a temperature of 200^0C. The experimental specimens of cobalt-bonded tungsten carbide used in the experiment were cut as rectangular block of 25×25×5 mm^3.

2.2 Experimental design

In order to identify the effects of aluminum powder particle on the machinability evaluation of cobalt-bonded tungsten carbide in the PM-EDM process, the following two factors of aluminum powder particle added dielectric were chosen for this study:

1. Grain size of aluminum powder particle (S_{Al} , μm);
2. Concentration of aluminum powder particle (C_{Al} , g/l).

The physical and mechanical properties of aluminum powder particle are a melting point of 933K, density of 2.73 g/cm^3, thermal conductivity of 2.38 W/cmK, electrical resistivity of 2.45 $\mu\Omega$cm and specific heat of 0.215 cal/gK.

In the EDM process, the most significant processing parameters includes the

workpiece polarity, pulse on time, pulse off time, open discharge voltage, discharge current, dielectric fluid and duty factor. Here the duty factor is the ratio of pulse on time to total pulse period. Table 1 shows the setting of experimental parameters in the PM-EDM process of 96WC-4Co. In this study, the discharge current (I_P, A) and pulse on time (τ_P, μs) were only taken into account as design factors for the finishing stages. The reason why these two factors have been chosen is that they are the most general and frequently used among EDM researchers [1-3]. At this moment, the electrode used in this study was subjected to a negative polarity.

Table 1 The EDM operating conditions

Working conditions	Unit	Description
Workpiece		94WC-6Co(25×25×5 mm^3)
Electrode material		electrolytic copper (ϕ10mm)
Electrode polarity		negative
Working time	mim	15
open discharge voltage	V	110
discharge current (I_P)	A	1.5 – 3.5
pulse on time (τ_P)	μs	50 – 250
Duty factor		0.75
Dielectric fluid		mineral oil (TOTAL EDM44)
Grain size of Al powder (S_{Al})	μm	1 – 3
Concentration of Al powder (C_{Al})	g/l	5 – 25

In this study, these four processing parameters, including the grain size (S_{Al}) and concentration (C_{Al}) of aluminum powder particle, discharge current (I_P) and pulse on time (τ_P), were chosen as the independent input variables in the analysis of RSM. In the experimental design, the experimental plans were designed on the basis of the central composite design (CCD) technique. The factorial portion of CCD is a full factorial design with all combinations of the factors at two levels (high, +2 and low, – 2) and composed of the eight star points and the six central points (coded level 0) which are the midpoint between the high and low levels. The star points are at the face of the cube portion on the design that corresponds to an α value of 2 and this type of design is

commonly called the "face-centered CCD". In this study, the experimental plan was conducted using the stipulated conditions according to the face-centered CCD and it involved a total of 30 experimental observations at four independent input variables. Each combination of experiments was carried out two times at different time under the same conditions to acquire a more accurate result in the PM-EDM process. The machining period for each experimental specimen is 15 min.

The low and high levels selected for the grain size (S_{Al}) and concentration (C_{Al}) of aluminum powder particle, discharge current (I_P) and pulse on time (τ_P) were: 1 and 3 μm, 5 and 25 g/l, 1.5 and 3.5 A, and finally, 50 and 250 μs, respectively. Table 2 shows both coded and actual value of the four process parameters and their ranges. The experimental matrix adopted in this study in the coded form is shown in Table 3. The coded values $X_{i,i=1,2,3,4}$ of the processing parameter used in Table 2 and 3 were obtained from the following transformable equations:

$$X_1 = \frac{S_{Al} - S_{Al0}}{\Delta S_{Al}} \tag{1}$$

$$X_2 = \frac{C_{Al} - C_{Al0}}{\Delta C_{Al}} \tag{2}$$

$$X_3 = \frac{I_P - I_{P0}}{\Delta I_P} \tag{3}$$

$$X_4 = \frac{\tau_P - \tau_{P0}}{\Delta \tau_P} \tag{4}$$

where X_1, X_2, X_3 and X_4 are the coded values of parameters S_{Al}, C_{Al}, I_P and τ_P, respectively. S_{Al0}, C_{Al0}, I_{P0} and τ_{P0} are the values of S_{Al}, C_{Al}, I_P and τ_P at zero level. ΔS_{Al}, ΔC_{Al}, ΔI_P and $\Delta \tau_P$ are the intervals of variation in S_{Al}, C_{Al}, I_P and τ_P, respectively.

Table 2 Design scheme of processing parameters and their levels

Parameters	Unit	Levels				
		− 2	− 1	0	+1	+2
Grain size of Al powder (S_{Al}), X_1	μm	1	1.5	2	2.5	3
Concentration of Al powder(C_{Al}), X_2	g/l	5	10	15	20	25
discharge current (I_P), X_3	A	1.5	2	2.5	3	3.5
pulse on time (τ_P), X_4	μs	50	100	150	200	250

2.3 Performance evaluations

The machining performance evaluations selected for this study were the material removal rate (MRR), the electrode wear ratio (EWR) and the surface roughness (SR). Both the values of MRR and EWR refer to the machining efficiency of the PM-EDM process and the wear of copper electrode, respectively, and are defined as follows:

$$\text{MRR(g/min)} = \frac{\text{wear weight of workpiece}}{\text{time of machining}} \tag{5}$$

$$\text{EWR(\%)} = \frac{\text{wear weight of electrode}}{\text{wear weight of workpiece}} \times 100\% \tag{6}$$

Workpiece and electrode was weighed before and after each experiment, using electric balance (Sartarus) with a resolution of 0.01 mg, to determine the value of MRR and EWR.

The surface roughness measurements for the machined surface are performed with a Mitutoyo SurfTest-402. The maximum surface roughness (Rmax, μm) was used to evaluate the surface roughness (SR) of the machined surface. For the efficient evaluations of the PM-EDM process, the larger value of MRR and the smaller both values of EWR and SR are regarded as the best machining performance. Therefore, the value of MRR is regarded as a “the larger-the-better characteristic”, and both values of EWR and SR are regarded as “the smaller-the-better characteristics” in this study.

Table 3 Design layout and experimental results

Run	coded factors				actual factors				Response variables		
	X_1	X_2	X_3	X_4	S_{Al}	C_{Al}	I_P	τ_P	MRR (g/min)	EWR (%)	SR (μm)
1	+1	+1	− 1	− 1	2.5	20	2	100	0.12205	17.26	2.43
2	+1	+1	+1	− 1	2.5	20	3	100	0.13105	19.85	3.03
3	0	0	0	0	2	15	2.5	150	0.16312	23.53	4.36
4	0	+2	0	0	2	25	2.5	150	0.13156	27.34	2.63
5	+1	− 1	− 1	+1	2.5	10	2	200	0.11235	24.57	6.82
6	− 1	+1	+1	+1	1.5	20	3	200	0.13143	23.94	2.93
7	0	0	0	− 2	2	15	2.5	50	0.15342	16.61	2.39
8	− 1	− 1	+1	− 1	1.5	10	3	100	0.07985	25.14	6.12
9	− 1	− 1	− 1	+1	1.5	10	2	200	0.08102	26.89	6.23
10	0	0	0	0	2	15	2.5	150	0.16278	23.54	4.32
11	+1	− 1	+1	+1	2.5	10	3	200	0.13154	24.68	6.92
12	0	− 2	0	0	2	5	2.5	150	0.07231	22.23	4.21
13	0	0	0	0	2	15	2.5	150	0.16342	23.52	4.33
14	0	0	− 2	0	2	15	1.5	150	0.14234	16.77	5.22
15	0	0	+2	0	2	15	3.5	150	0.16591	27.37	6.92
16	− 1	+1	+1	− 1	1.5	20	3	100	0.12685	21.44	2.74
17	− 1	+1	− 1	− 1	1.5	20	2	100	0.12485	19.44	2.22
18	+2	0	0	0	3	15	2.5	150	0.16770	26.65	6.82
19	− 1	− 1	− 1	− 1	1.5	10	2	100	0.07785	23.12	5.34
20	0	0	0	0	2	15	2.5	150	0.16366	23.53	4.28
21	− 1	+1	− 1	+1	1.5	20	2	200	0.13254	21.62	2.65
22	− 1	− 1	+1	+1	1.5	10	3	200	0.09231	22.99	6.45
23	0	0	0	+2	2	15	2.5	250	0.17235	27.37	3.51
24	+1	− 1	+1	− 1	2.5	10	3	100	0.08405	20.77	6.73
25	+1	− 1	− 1	− 1	2.5	10	2	100	0.07205	17.29	6.48
26	+1	+1	− 1	+1	2.5	20	2	200	0.13541	21.02	2.83
27	0	0	0	0	2	15	2.5	150	0.16243	23.51	4.21
28	+1	+1	+1	+1	2.5	20	3	200	0.14312	21.65	3.26
29	0	0	0	0	2	15	2.5	150	0.16372	23.55	4.24
30	− 2	0	0	0	1	15	2.5	150	0.15923	15.98	5.76

3. Response surface modeling

The RSM was employed for the modeling and analysis of processing parameters in the PM-EDM process in order to obtain the relationship to the material removal rate (MRR), electrode wear ratio (EWR) and surface roughness (SR). In the RSM, the quantitative form of relationship between desired response and independent input variables can be represented in the following:

$$Y = f(S_{Al}, C_{Al,} I_P, \tau_P) \tag{7}$$

where Y is the desired response and f is the response function (or response surface). In the procedure of analysis, the approximation of Y was proposed by using the fitted second order polynomial regression model which is called the quadratic model. The quadratic model was exactly suitable for studying carefully the interactive effects of combinative factors on the performance evaluations [16-20]. The quadratic model of Y can be written as following: The appearance of response function is a surface as plotting the expected response of f . The identification of suitable approximation of f will determine whether the application of RSM is successful or not. In this study, the approximation of f was proposed using the fitted second order polynomial regression model, which called the quadratic model. The desired quadratic response (Y) is always described as follows.

$$Y = a_0 + \sum_{i=1}^{4} a_i X_i + \sum_{i=1}^{4} a_{ii} X_i^2 + \sum_{i<j}^{4} a_{ij} X_i X_j \tag{8}$$

where a_0 is constant, a_i, a_{ii} and a_{ij} represent the coefficients of linear, quadratic and cross product terms, respectively. X_i reveals the coded variables corresponding to the studied machining parameters. The material removal rate (MRR), electrode wear ratio (EWR), and surface roughness (SR), indicated as Y_1, Y_2 and Y_3, respectively, were analyzed. Using the quadratic model of f in this study not only aims to investigate the response over the entire factor space, but also aims to locate the region of the desired target where the response approaches its optimum or near-optimal value.

RSM is a sequential procedure and its procedure for modeling and analysis of the

effects of process parameters on the performance characteristics in the PM-EDM process of 96WC-4Co including six steps is summarized as following:

(1) Defining the independent input variables and desired responses with the design constraints.
(2) Adopting the face-centered CCD to plan the experimental design.
(3) Performing regression analysis with the quadratic model of RSM.
(4) Calculating the statistical analysis of variance (ANOVA) for the independent input variables and finding which parameter significantly affects the desired response.
(5) Determining the situation of the quadratic model of RSM and deciding whether the model of RSM needs screening variables or no.

Conducting confirmation experiment and verifying the predicted performance characteristics.

4. Results and discussion

The 30 experimental runs were conducted in duplicate, and the average values of material removal rate (MRR), electrode wear ratio (EWR), and surface roughness (SR) along with the design matrix are listed in Table 3

4.1 ANOVA analysis of the final quadratic models for MR, EWR and SR

In order to ensure the goodness of fit of the quadratic model obtained in this study, the test for significance of the regression model, the test for significance on individual model coefficients and the test for lack-of-fit need to be performed [20]. These tests are performed as ANOVA procedure by calculating the "*F*-value", the "*Prob. > F*", the determination coefficients (R^2) and the adequate precision (*AP*). The values of "*F*-value" and the "*Prob. > F*" imply statistical significance on the regression model and the particular linear, quadratic or interaction terms. Usually the desired confidence level be set to 95%, the value of "*Prob. > F*" smaller than 0.05 signify that the regression model is considered to be statistically significant, which is desirable as it demonstrates that the terms in the model have a significant effect on the responses. The determination coefficient R^2 is defined as the ratio of the explained variation to the total variation and is a measure of the degree of fit. When R^2 approaches unity, the better the response model fits the actual data, It exists the less the difference between the

predicted and actual values. Furthermore, the value of adequate precision (AP) in this model, which compares the range of the predicted value at the design point to the average prediction error, is well above 4. The value of the ratio is greater than 4, which presents the adequate model discrimination. These models obtained present higher values of the determination coefficients (R^2) and adequate precision (AP) at the same time. In Table 4, the model fitting assessment for the quadratic model of MR, EWR and SR is based on statistical parameters above. From the results of Table 4, these obtained quadratic models of MRR, EWR and SR can be regard as significant effect for fitting and predicting the experimental results and meantime the test of lack-of-fit also displays to be insignificant.

Table 4 Response surface model evaluation

Model	Y_1 (MRR)	Y_2 (EWR)	Y_3 (SR)
Model degree	Quadratic	Quadratic	Quadratic
F-value	8.779857	23.082666	6.353939
Prob. $>F$	< 0.0001	< 0.0001	0.0005
R^2	0.914544	0.956514	0.955707
Adj- R^2	0.901452	0.938589	0.921033
AP	7.956731	12.830365	9.882709
Standard deviation	0.214097	1.412086	0.865038
Lack of Fit	Not significant	Not significant	Not significant
Significant model terms	$X_1, X_2, X_3, X_4, X_1^2, X_2^2, X_3^2, X_1X_3, X_2X_4$	$X_1, X_2, X_3, X_4, X_1^2, X_2^2, X_4^2, X_1X_4, X_2X_4$	$X_1, X_2, X_3, X_4, X_2^2, X_4^2, X_1X_4, X_2X_3, X_2X_4$

The significant model terms are also summarized in Table 4. In the case of Y_1 (MRR), the $X_1(S_{Al})$, $X_2(C_{Al})$, $X_3(I_P)$, $X_4(\tau_P)$, X_1^2, X_2^2, X_3^2, X_1X_3 and X_2X_4 can be regard as significant terms due to their "Prob. > F" value being less than 0.05. Similarly, the $X_1(S_{Al})$, $X_2(C_{Al})$, $X_3(I_P)$, $X_4(\tau_P)$, X_1^2, X_2^2, X_4^2, X_1X_4 and X_2X_4 for the Y_2 (EWR), and the $X_1(S_{Al})$, $X_2(C_{Al})$, $X_3(I_P)$, $X_4(\tau_P)$, X_2^2, X_4^2, X_1X_4, X_2X_3 and X_2X_4 for the Y_3 (SR) are the significant terms. The

backward elimination process eliminates the insignificant terms to adjust the fitted quadratic models. These insignificant model terms can be removed and the test of lack-of-fit also displays to be insignificant. Through the backward elimination process, the final quadratic models of response equation in terms of coded factors are presented as follows:

・the material removal rate (MRR, g/min)

$$\begin{aligned} Y_1 &= 0.156538 + 0.004244\,X_1 + 0.018115\,X_2 + 0.004550\,X_3 \\ &+ 0.007457\,X_4 - 0.004842\,X_1^2 - 0.020225\,X_2^2 - 0.007177\,X_3^2 + 0.0 \\ &02107\,X_1X_3 - 0.004107\,X_2X_4 \end{aligned} \tag{9}$$

・the electrode wear ratio (EWR, %)

$$\begin{aligned} Y_2 &= 23.006071 + 0.160416\,X_1 - 0.375416\,X_2 + 1.26875\,X_3 \\ &+ 1.857083\,X_4 - 0.581696\,X_1^2 + 0.285803\,X_2^2 - 0.412946\,X_4^2 \\ &+ 0.653125\,X_1X_4 - 0.160625\,X_2X_4 \end{aligned} \tag{10}$$

・the surface roughness (SR, μm)

$$\begin{aligned} Y_3 &= 5.19875 + 0.2475\,X_1 - 1.34\,X_2 + 0.274166\,X_3 \\ &+ 0.218333\,X_4 - 0.349218\,X_2^2 - 0.466718\,X_4^2 - 0.0425\,X_1X_4 \\ &+ 0.03\,X_2X_3 - 0.03125\,X_2X_4 \end{aligned} \tag{11}$$

In terms of actual factors, the final quadratic models of response equation are as follows:

・the material removal rate (MRR, g/min)

$$\begin{aligned} Y_1 &= -0.393672 + 0.064893\,S_{Al} + 0.030357\,C_{Al} + 0.135791\,I_P \\ &+ 0.000395 \\ &\tau_P - 0.01937\,S_{Al}^2 - 0.000809\,C_{Al}^2 - 0.02871\,I_P^2 \\ &+ 0.00843\,S_{Al}\,I_P - 0.000016\,C_{Al}\,\tau_P \end{aligned} \tag{12}$$

・the electrode wear ratio (EWR, %)

$$\begin{aligned} Y_2 &= 7.516101 + 5.709226\, S_{Al} - 0.321672\, C_{Al} + 2.5375\, I_P \\ &+ 0.044082\, \tau_P - 2.326785\, S_{Al}^{\,2} + 0.011432\, C_{Al}^{\,2} - 0.000165\, \tau_P^{\,2} \\ &+ 0.026125\, S_{Al}\, \tau_P - 0.000642\, C_{Al}\, \tau_P \end{aligned} \quad (13)$$

· the surface roughness (SR, μm)

$$\begin{aligned} Y_3 &= -1.481770 + 0.75\, S_{Al} + 0.139812\, C_{Al} + 0.368333\, I_P \\ &+ 0.065647\, \tau_P - 0.013968\, I_P^{\,2} - 0.000186\, \tau_P^{\,2} - 0.0017\, S_{Al}\, \tau_P \\ &+ 0.012\, C_{Al}\, I_P - 0.000125\, C_{Al}\, \tau_P \end{aligned} \quad (14)$$

The above mathematical model can be used for predicting the values of MRR, EWR, and SR within the limits of the factors studied. The differences between the measured and predicted response are illustrated in Figure 1, 2, and 3. From the results of comparison, it proved that the predicted values of MRR, EWR and SR are close to those readings recorded experimentally with a 95% confidence interval.

4.2 The effect of powder particles on discharge mechanism

Under a series of recurring electrical spark, the powder particles located between the electrode and workpiece get energized and behave in a zigzag fashion. Due to the interlocking between the different powder particles, these particles will display in the form of chain at different places under the sparking area [8-15]. This chain formation improves in bridging the gap between both the electrodes, and decreases the gap voltage and the insulating strength of dielectric fluid. As a result, the “series discharge” within a discharge easily takes place, which disperse a discharge energy effect under the sparking area. Figure 4 depicts various discharging waveforms with different concentrations (C_{Al}) of aluminum powder particle. The discharging wave form is consistent with the input in the case of mineral oil without being added aluminum powder particle, as shown in Figure 4(a). However, the dielectric fluid with aluminum powder particle, the responded waveforms are entirely different from the primary input pulse, as shown in Figure 4(b) and 4(c). These waveforms display multiple discharging effects within a single input pulse. This occurs as a result of discharging energy dispersion under the sparking area.

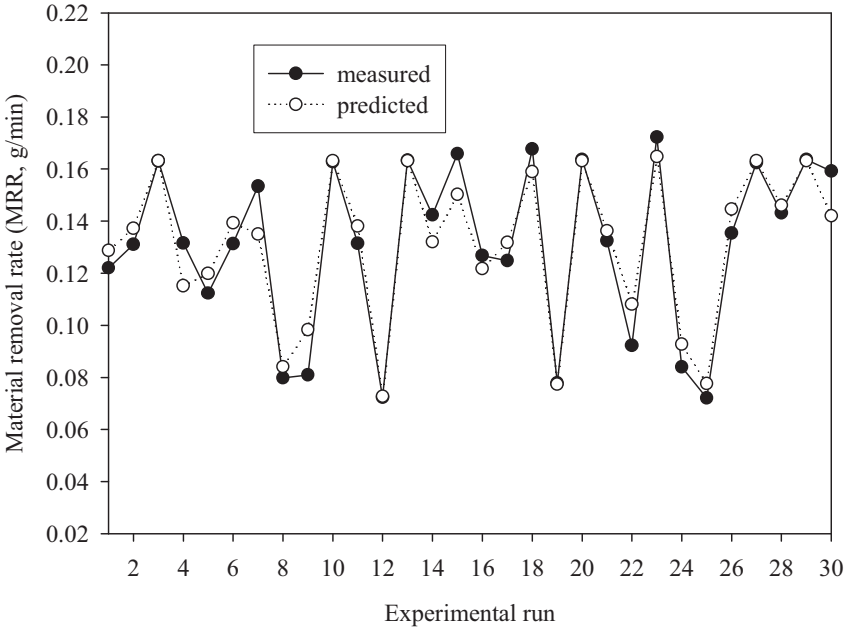

Figure 1 Comparison of measured and predicted value for material removal rate (MRR, g/min)

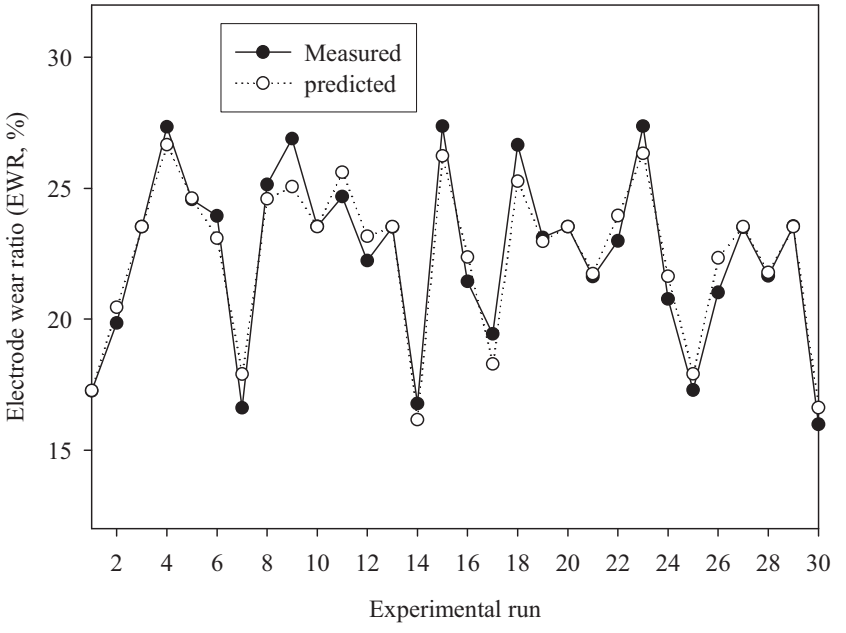

Figure 2 Comparison of measured and predicted value for electrode wear rate (EWR, %)

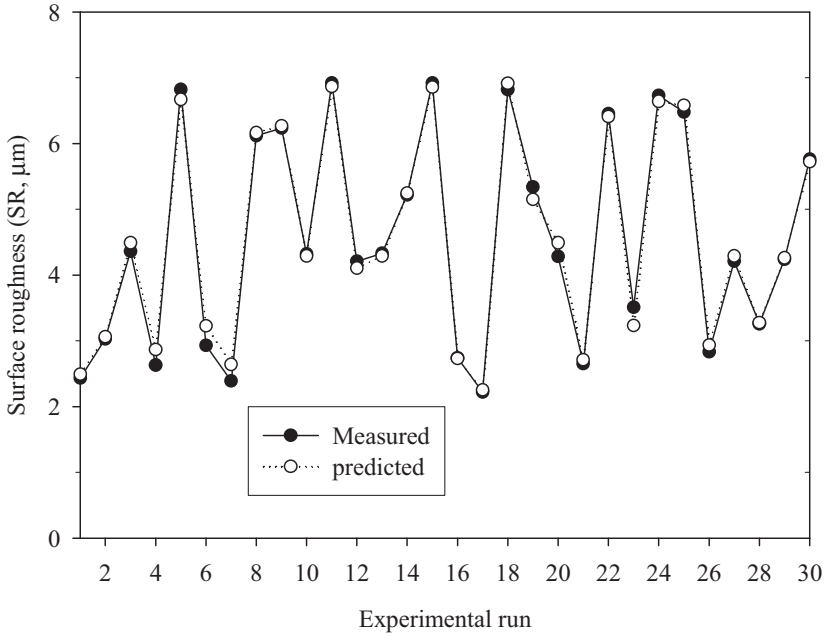

Figure 3 Comparison of measured and predicted value for surface roughness (SR, μm)

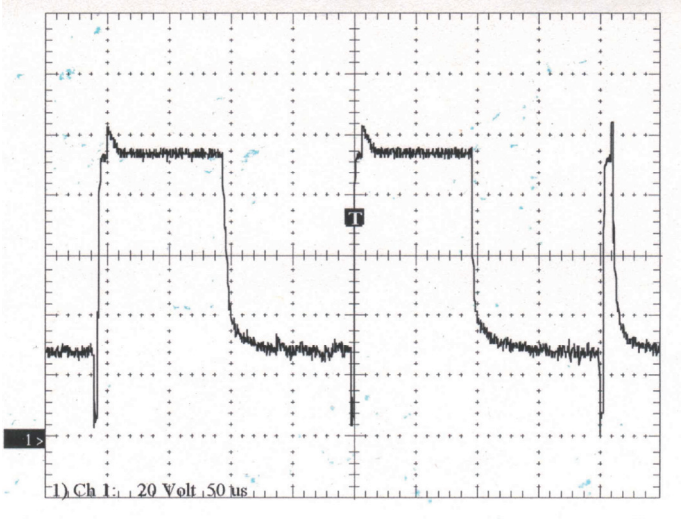

(a)

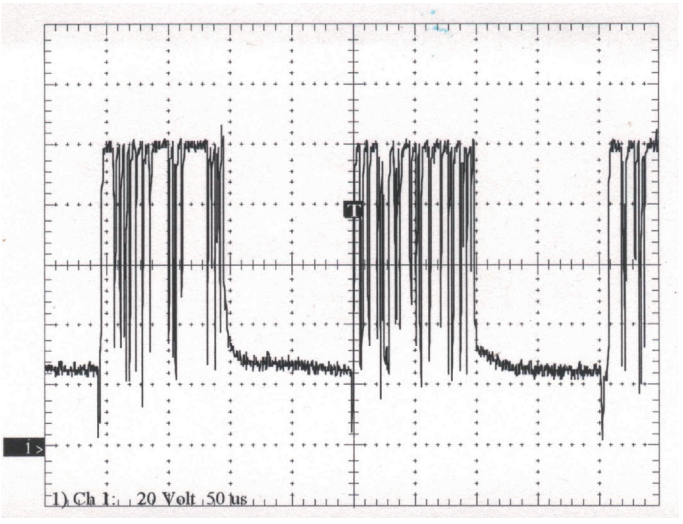

(b)

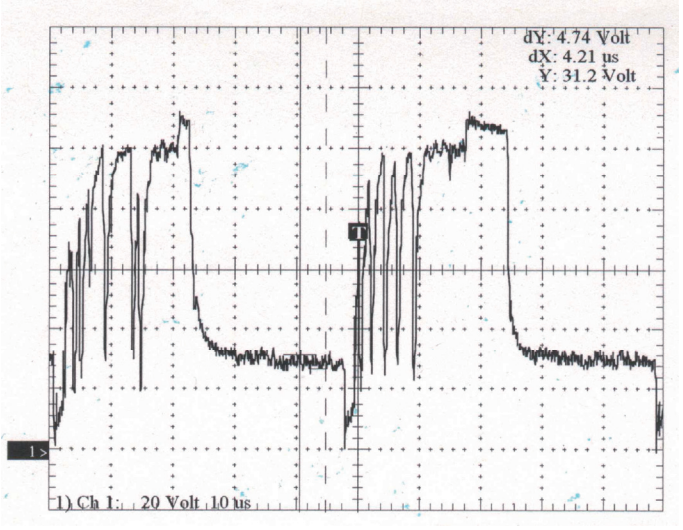

(c)

Figure 4 Discharging waveform of voltage using (a) pure mineral oil, (b) mineral oil added 5 g/l of powder concentration and (c) mineral oil added 25 g/l of powder concentration

4.3 Response surface and contour plots of the variation of thickness

As for the EDM process, the electrical spark-erosion process occurred successively, and then the removal of melt took place in the form of crater on the machined surface. The amount of melt removal determines the degree of material removal rate (MRR). Figure 5 shows the estimated response surface for the MRR in relation to the processing parameters of grain size (S_{Al}) and concentration (C_{Al}) of aluminum powder particle, with the discharge current (I_P) and pulse on time (τ_P) keeping at the middle level. As shown in the figure, while aluminum powder concentration was increased, it will help to bridge the gap between the electrode and workpiece with the result that the material removal rate (MRR) increases. This is because the bridging effect generates the multiple discharging effects within a single input pulse, the frequency of discharging increases. So the faster sparking within a single input pulse takes place, and this causes faster erosion from the workpiece surface. In Figure 5, it can be found that an overly high concentration, whatever the grain size is, would reduce the value of MRR and display a discharge interference phenomenon. The optimal material removal rate would appear at the aluminum powder concentration 20 g/l. In addition, the above-mentioned effects of adding aluminum powder concentration have an identical trend of MRR influences for various grain size of aluminum powder particle. From Figure 5, the value of MRR is shown to generally increase with increase of grain size, up to 2.5 μm , and then slightly decrease with a further increase in the grain size.

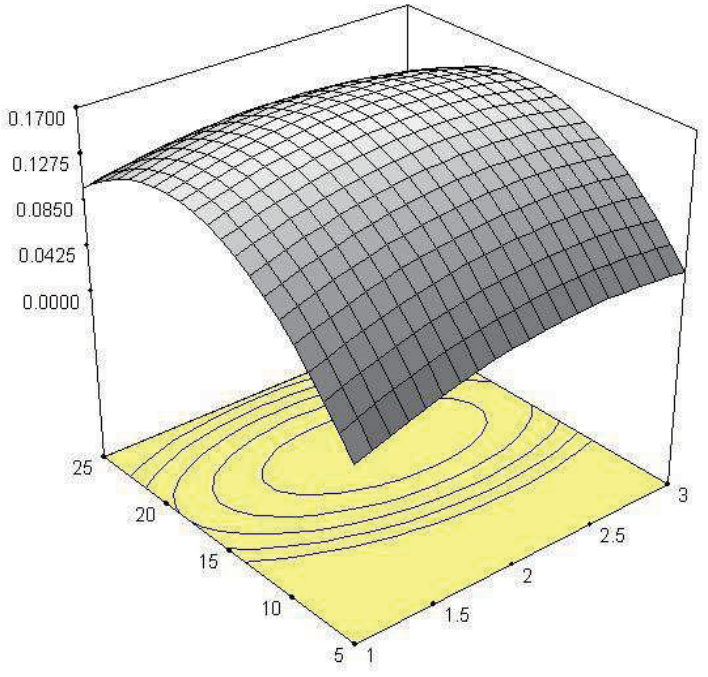

Figure 5 The estimated response surface for the material removal rate (MRR) according to change of grain size (S_{Al}) and concentration (C_{Al}) of aluminum powder particle with the discharge current (I_P =2.5A) and pulse on time (τ_P =150 μ s) keeping at the middle level.

Figure 6 depicts the effects of discharge current (I_P) and pulse on time (τ_P) on the value of MRR under the grain size of 2 μ m and powder concentration of 15 g/l. The value of MRR is shown to continually increase with an increase of discharge current since the higher spark energy produces more and bigger craters on the machined surface, and this will result in higher material removal. In Figure 6, the value of MRR is also shown to generally increase with an increase of pulse on time, up to 200 μ s , and then slightly decreases with a further increase in the pulse on time. This event has been attributed to the increase of input energy in the high pulse on time, which results in more debris on the gap between the workpiece and the electrode, and hence it creates a short circuit and decreases the efficiency of electrical spark-erosion.

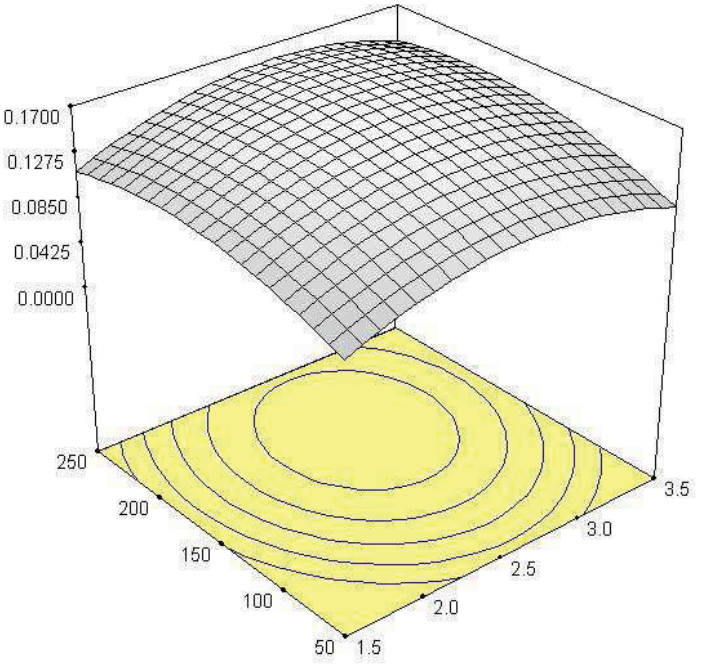

Figure 6 The estimated response surface for the material removal rate (MRR) according to change of discharge current (I_P) and pulse on time (τ_P) with the grain size ($S_{Al} = 2\,\mu$m) and concentration ($C_{Al} = 15$g/l) of aluminum powder particle keeping at the middle level.

4.4 The effect of processing parameters on the EWR

The electrode wear of EDM process includes corner wear, side wear, and end wear. The status of electrode wear affects the dimensional accuracy of machined components since the die-sinking EDM process is the projection manufacture. Figure 7 shows the estimated response surface for the EWR in relation to the processing parameters of grain size (S_{Al}) and concentration (C_{Al}) of aluminum powder particle, with the discharge current (I_P) and pulse on time (τ_P) keeping at the middle level.

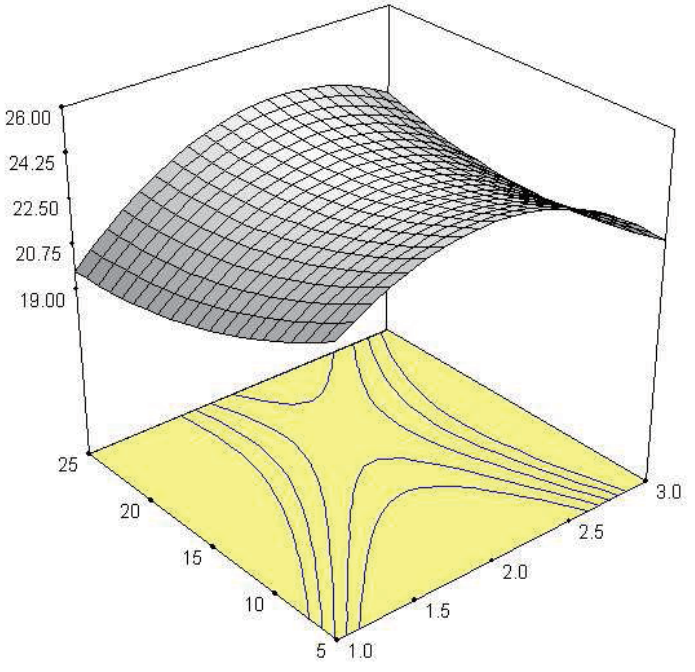

Figure 7 The estimated response surface for the electrode wear ratio (EWR) according to change of grain size (S_{Al}) and concentration (C_{Al}) of aluminum powder particle with the discharge current (I_P=2.5A) and pulse on time (τ_P=150 μs) keeping at the middle level.

The value of EWR is shown to quickly increase with an increase of grain size. As mentioned above, the dielectric fluid with conductive powder added could improve the efficiency of discharging and display higher electrode wear. However, the increase is diminished after 2.5 μm and the value of EWR decreases with a further increase in the grain size. Because the spark gap is filled up with larger amount of removed debris and big grains also cause short circuit, the efficiency of electrical spark-erosion decreases. In addition, the value of EWR, whatever the grain size is, generally increases with an increase of powder concentration. In general, the workpiece machined with dielectric fluid plus aluminum powder not only creates a large value of MRR, but also presents a relatively large value of EWR.

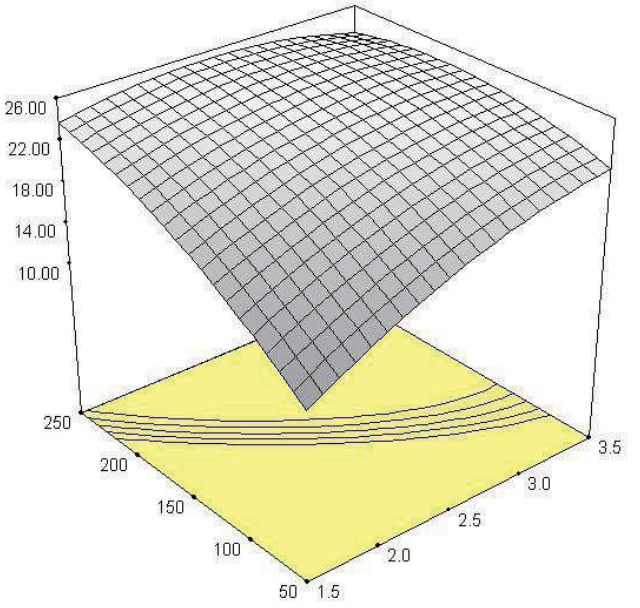

Figure 8 The estimated response surface for the electrode wear ratio (EWR) according to change of discharge current (I_P) and pulse on time (τ_P) with the grain size ($S_{Al} = 2\,\mu$m) and concentration ($C_{Al} = 15$g/l) of aluminum powder particle keeping at the middle level.

Figure 8 shows the effects of discharge current (I_P) and pulse on time (τ_P) on the value of EWR under the grain size of $2\,\mu$m and powder concentration of 15 g/l. The value of EWR is shown to quickly increase with an increase of pulse on time. In Figure 8, it can also be seen that the value of EWR increases with an increase of the discharge current. A large released discharging energy and a better peak current density, driven by discharge current and pulse on time, can exhibit the large EWR.

4.5 The effect of processing parameters on the SR

The dielectric fluid with conductive powder added could enlarge the spark gap distance between the electrode and workpiece increasing from 25-50 to 50-150 μm [7-10]. The plasma channel is modified to become enlarged and widened simultaneously. The result of discharging energy dispersion reveals that more uniform distribution of the discharge takes place among the powder particles under the sparking

area. Therefore, the uniform erosion forming the workpiece surface decreases the crater diameter, the depth and melted material overflow. The smaller amount of removed debris and shallow craters are obtained, and perform a better surface roughness on the machined surface of workpiece. Figure 9 illustrates the effects of grain size (S_{Al}) and concentration (C_{Al}) of aluminum powder particle on the value of SR under the discharge current (I_P) of 2.5 A and pulse on time (τ_P) of 150 μs . Obviously, the value of SR is shown to continually decrease with an increase of powder concentration. But the value of SR is shown to increase with an increase of grain size for various powder concentrations. This result has been attributed to large amount of big grain filled up the sparking gap, which causes a bridging effect. This bridging effect results in more concentrated discharging energy so that it produces an increase of the diameter and the depth of craters on the machined surface. Hence the surface roughness consequently increases.

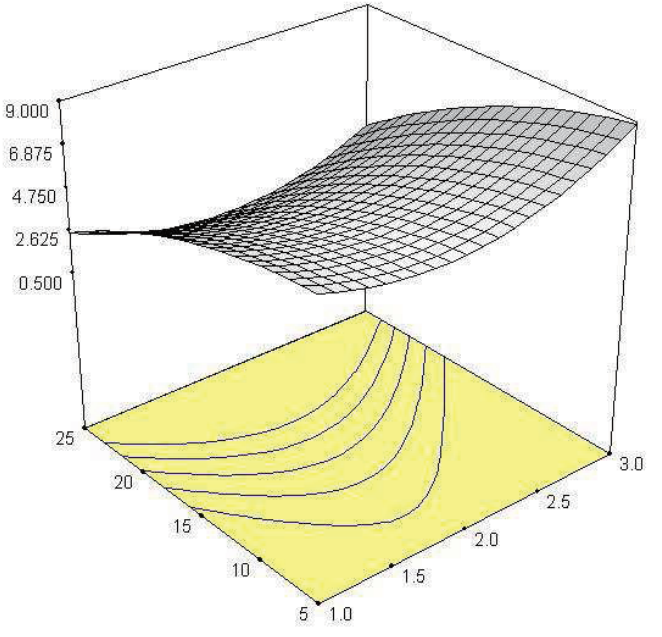

Figure 9 The estimated response surface for the surface roughness (SR) according to change of grain size (S_{Al}) and concentration (C_{Al}) of aluminum powder particle with the discharge current (I_P =2.5A) and pulse on time (τ_P =150 μs) keeping at the middle level.

The surface roughness on the machined surface is subjected to the various diameter and depth of discharge craters generated by consecutive electrical discharge. Therefore, the value of MRR increases with the increase of pulse on time, in the meantime, the surface roughness increases with the increase of large and deep craters formed on the machined surface. Figure 10 depicts the effects of discharge current (I_P) and pulse on time (τ_P) on the value of SR under the grain size of 2 μm and powder concentration of 15 g/l. The increase of discharge current increases the surface roughness, as shown in Figure 10, due to an increase of the diameter and the depth of craters.

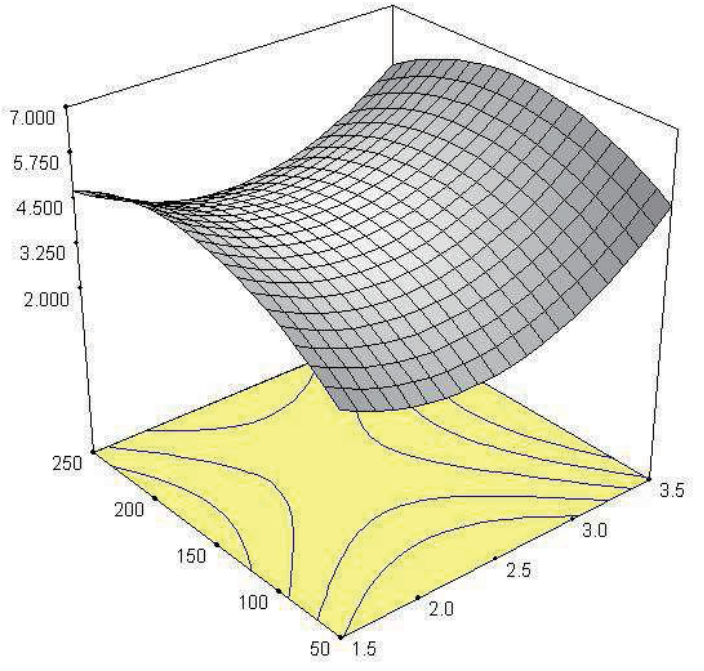

Figure 10 The estimated response surface for the surface roughness (SR) according to change of discharge current (I_P) and pulse on time (τ_P) with the grain size (S_{Al} = 2 μm) and concentration (C_{Al} = 15g/l) of aluminum powder particle keeping at the middle level.

However, the SR value first increases with an increase of pulse on time before 200 μs and then decreases with a further increase in the pulse on time. When the pulse on time is set on high level, the discharge energy density is reduced on the electrical discharge spot and the rapidly resolidified phenomenon of machined surface appears

successively. Consequently, the surface roughness of machined surface decreases when the pulse on time is increased. Hence the machined surface is impacted and this will results in higher surface roughness at the high value of pulse on time.

5. Conclusions

This study concentrates the quantitative analysis of machinability evaluation of cobalt-bonded tungsten carbide by PM-EDM process. Mathematical models of the MRR, EWR and SR had been carried out to correlate the dominant processing parameters, including the grain size, concentration of aluminum powder particle, discharge current and pulse on time, on the machinability evaluation of cobalt-bonded tungsten carbide. An experimental plan of the face centered CCD based on the RSM has been employed to carry out the experimental study. Conclusions are summarized as follows.

(1) The results of ANOVA and comparisons of experimental data represent that the mathematical models of the value of MRR, ERW and SR are fairly well fitted with the experimental values with a 95% confidence interval.

(2) Using dielectric fluid with conductive aluminum powder added can effectively disperse and uniform the discharging energy dispersion in order to refine the machined surface roughness.

(3) The aluminum powder particles suspended in the dielectric fluid affect the MRR, EWR and SR in the PM-EDM process. Both the values of MRR and EWR increase with the increase of the grain size and concentration of aluminum powder. In addition, the value of SR decreases with an increase of powder concentration, and increase with an increase of grain size for various powder concentrations.

(4) Both the values of MRR and EWR increase with the increase of the discharge current and pulse on time. The value of SR first decreases with the increase of pulse on time before 200 μs and then increases with a further increase in the pulse on time.

References

[1] Snoeys, R., Staelens, F., and Dekeyser, W. (1986), Current trends in nonconventional material removal processes. Ann. CIRP, 35(2), 467-476.

[2] McGeough, J. A. (1988), Advanced Methods of Machining. Chapman & Hall, New York.

[3] Kahng, C. H. and Rajurkar, K. P. (1997), Surface characteristics behaviour due to rough and fine cutting by EDM. Ann. CIRP, 25(1), 77–82.

[4] Kruth, J. P. and Stevens, L. (1995), Study of the white layers of a surface machined by die-sinking electro-discharge machining. Ann. CIRP, 44(1), 169–172.

[5] Rebelo, J. C. (1998), Influence of EDM pulse energy on the surface integrity of martensitic steels. J Mater Process Technol, 84(1), 90–96.

[6] Erden, A. and Bilgin, S. (1980), Role of impurities in electric discharge machining. Proceedings of the 21st International Machine Tool Design and Research Conference, Macmillan, London, p 345–350

[7] Jeswani, M. L. (1981). Effects of the addition of graphite powder to kerosene used as the dielectric fluid in electrical discharge machining. Wear, 70, 133–139.

[8] Mohri, N., Saito, N. M. and Higashi, A. A. (1991), New process of finish machining on free surface by EDM methods. Ann. CIRP 40(1), 207–210.

[9] Yan, B. H. and Chen, S. L. (1994), Characteristics of SKD11 by complex process of electric discharge machining using liquid suspended with aluminum powder. J Jpn Inst Light Met, 58 (9), 1067–1072.

[10] Uno, Y. and Okada, A. (1997), Surface generation mechanism in electrical discharge machining with silicon powder mixed fluid. Int J Electro Mach, 2, 13–18.

[11] Wong, Y. S., Lim, L. C., Rahuman, I. and Tee, W. M. (1998), Near-mirror-finish phenomenon in EDM using powder-mixed. J Mater Process Technol, 79(1), 30–40.

[12] Furutani, K., Saneto, A., Takezawa, H., Mohri, N. and Miyake, H. (2001), Accertation of titanium carbide by electrical discharge machining with powder suspended in working fluid. Prec Eng, 25, 138–144.

[13] Yan, B. H., Lin, Y. C., Huang, F. Y. and Wang, C. H. (2001), Surface modification of SKD 61 during EDM with metal powder in the dielectric. Mater Trans, 42(12),

2597–2604.

[14] Wu, K. L., Yan, B. H., Huang, F. Y. and Chen, S. C. (2005), Improvement of surface finish on SKD steel using electro-discharge machining with aluminum and surfactant added dielectric. Int J Mach Tools Manufact, 45, 1195–1201.

[15] Kansal, H. K., Singh,S. and Kumara, P. (2005), Parametric optimization of powder mixed electrical discharge machining by response surface methodology. J Mater Process Technol, 169(2), 385–391.

[16] Myers, R. H. and Montgomery, D. H. (1995), Response Surface Methodology. John Wiley & Sons, USA.

[17] Grum,J. and Slab, J. M. (2004), The use of factorial design and response surface methodology for fast determination of optimal heat treatment conditions of different Ni–Co–Mo surface layers. J Mater Process Technol, 155–156, 2026–2032.

[18] Ozcelik, B. and Erzurmlu, T. (2005), Determination of effecting dimensional parameters on warpage of thin shell plastic parts using integrated response surface method and genetic algorithm. Int Commun Heat Mass Transf , 32, 1085–1094.

[19] Oktem, H., Erzurmlu, T. and Kurtaran, H. (2005), Application of response surface methodology in the optimization of cutting conditions for surface roughness. J Mater Process Technol, 170(1), 11–16.

[20] Fisher, R. A. (1925), Statistical method for research worker. Oliver & Boyd, London.